JPET Fast Forward. Published on October 16, 2007 as DOI: 10.1124/jpet.107.127266

Inhibition of N-type calcium channels by activation of GPR35, an orphan receptor, heterologously expressed in rat sympathetic neurons

Juan Guo, Damian J. Williams, Henry L. Puhl 3rd, and Stephen R. Ikeda

Section on Transmitter Signaling

Laboratory of Molecular Physiology

National Institute on Alcohol Abuse and Alcoholism

National Institutes of Health

Bethesda, MD 20892 USA

Running title: **Modulation of N-type calcium channels via GPR35**

Corresponding author: Stephen R. Ikeda

Section on Transmitter Signaling, Laboratory of Molecular Physiology

NIH/NIAAA

5625 Fishers Lane, MSC 9411

Bethesda, MD 20892-9411 (regular mail)

Rockville, MD 20852 (express mail)

Tel: (301) 433-2807

Fax: (301) 480-0466

Email: sikeda@mail.nih.gov

Number of text pages: 31

Number of tables: 0

Number of figures: 6

Number of references: 37

Number of words in the abstract: 224

Number of words in the introduction: 687

Number of words in the discussion: 1153

ABBREVIATIONS: KYNA, kynurenic acid, 4-oxo-1H-quinoline-2-carboxylic acid; zaprinast, 1,4-dihydro-5-(2-propoxyphenyl)-7H-1,2,3-triazolo[4,5-d]pyrimidine-7-one; PTX, *Bordetella pertussis* toxin; SCG, superior cervical ganglion; BFR, basal facilitation ratio.

JPET Fast Forward. Published on October 16, 2007 as DOI: 10.1124/jpet.107.127266
This article has not been copyedited and formatted. The final version may differ from this version.

ABSTRACT

GPR35 is a G protein coupled receptor recently "de-orphanized" using high throughput intracellular calcium measurements in clonal cell lines expressing a chimeric G-protein α-subunit. From these screens, kynurenic acid, an endogenous metabolite of tryptophan, and zaprinast, a synthetic inhibitor of cyclic guanosine monophosphate specific phosphodiesterase, emerged as potential agonists for GPR35. To investigate the coupling of GPR35 to natively expressed neuronal signaling pathways and effectors, we heterologously expressed GPR35 in rat sympathetic neurons and examined the modulation of N-type ($Ca_V2.2$) calcium channels. In neurons expressing GPR35, calcium channels were inhibited in the absence of overt agonist indicating a tonic receptor activity. Application of kynurenic acid or zaprinast resulted in robust voltage-dependent calcium current inhibition characteristic of Gβγ-mediated modulation. Both agonist-independent and -dependent effects of GPR35 were blocked by *Bordetella pertussis* toxin pretreatment indicating the involvement of $G_{i/o}$ proteins. In neurons expressing GPR35a, a short splice variant of GPR35, zaprinast was more potent (EC_{50} = 1 μM) than kynurenic acid (58 μM), but had a similar efficacy (approximately 60% maximal calcium current inhibition). Expression of GPR35b, which has an additional 31 residues at the N-terminus, produced similar results but with much greater variability. Both GPR35a and GPR35b appeared to have similar expression patterns when fused to fluorescent proteins. These results suggest a potential role for GPR35 in regulating neuronal excitability and synaptic release.

JPET Fast Forward. Published on October 16, 2007 as DOI: 10.1124/jpet.107.127266
This article has not been copyedited and formatted. The final version may differ from this version.

Introduction

G protein-coupled receptors (GPCRs) comprise one of the largest families of cell surface proteins and represent a major target for both current therapeutics and drugs under development. Many cDNA clones are predicted to code for GPCRs based on high sequence similarity, especially in the transmembrane domains, to established GPCRs. For such orphan GPCRs, the identification of agonists, antagonists, and signal transduction pathways represents a major effort by industry for the discovery of novel drug targets (Stadel et al., 1997). GPR35, an orphan GPCR first discovered during a human genomic DNA screen, shares limited sequence homology with purinergic P2Y receptors, nicotinic acid receptor HM74, lysophosphatidic acid receptor GPR23, and an orphan receptor, GPR55. The highest levels of GPR35 mRNA were found in immune and gastrointestinal tissues with only limited expression in lung and neuronal tissues (O'Dowd et al., 1998; Wang et al., 2006). Subsequent to the initial description of GPR35 (now denoted GPR35a), Okumura et al. (2004) isolated a splice variant (GPR35b) from a human gastric cancer cDNA library that coded for an additional 31 amino acids at the N-terminus. GPR35a and GPR35b mRNA levels were up-regulated in gastric cancer tissue suggesting a role for both splice variants in malignant transformation. However, in the absence of an identified agonist, the functional role GPR35 plays in either normal or pathological states remains enigmatic.

Recently, using high throughput technology, kynurenic acid (KYNA; Wang et al., 2006) and zaprinast (Taniguchi et al., 2006) were identified as putative agonists for GPR35 by monitoring elevation of intracellular [Ca^{2+}] in cell lines co-expressing GPR35a and chimeric G-protein α-subunits. Kynurenic acid, an intermediate metabolite of tryptophan, is often used as a non-specific ionotropic glutamate receptor antagonist. Kynurenic acid is also a noncompetitive antagonist of the α7 nicotinic acetylcholine receptor that inhibits synaptic transmission in

cultured rat hippocampal neurons via both pre- and postsynaptic mechanisms (Hilmas et al., 2001). As a naturally occurring metabolite, KYNA potentially serves as an endogenous agonist for GPR35. The other identified agonist, zaprinast, is a synthetic inhibitor of cyclic guanosine monophosphate (cGMP) specific phosphodiesterases (PDE), especially PDE5 and PDE6. As a compound closely related to sildenafil (a clinically effective drug for erectile dysfunction), zaprinast has been used as diagnostic tool to identify signaling pathways involving cGMP generation and degradation (Gibson, 2001). However, zaprinast-mediated intracellular Ca^{2+} mobilization via GPR35a activation was found to be independent of cGMP degradation (Taniguchi et al., 2006).

Thus far, only artificial G proteins α-subunits (i.e., G_{qi5}, G_{qi9}, G_{qo5}, G_{qs5}) have been used to detect transduction signals following GPR35 activation (Wang et al., 2006; Taniguchi et al., 2006). In these high throughput systems, expression of a chimeric G protein α-subunit switches the coupling of $G_{i/o}$ and G_s preferring GPCRs to G_q (by altering residues in the c-terminus that convey receptor coupling specificity) thereby allowing changes in intracellular [Ca^{2+}] to be used as a readout for receptor activation. Although chimeric G α-subunits are useful for predicting GPCR coupling specificity, functional discrepancies between chimeric and native G protein-mediated effects have been reported (Kostenis et al., 2005). Therefore, a goal of the present study was to evaluate the function of GPR35 expressed within a context of unmodified G proteins at native expression levels. A second goal was to establish a model system for the future testing of novel agents, such as the endocannabinoid N-arachidonoyl L-serine (Milman et al., 2006), on GPR35 function. GPR35 shares significant sequence similarity with GPR55, an orphan GPCR that putatively binds cannabinoid ligands (Baker et al., 2006) but may not represent a classical cannabinoid receptor (Petitet et al., 2006). In the present study, we examined N-type

JPET Fast Forward. Published on October 16, 2007 as DOI: 10.1124/jpet.107.127266
This article has not been copyedited and formatted. The final version may differ from this version.

Ca^{2+} channel modulation in rat sympathetic neurons following GPR35 activation by KYNA or zaprinast. We found that both compounds inhibited N-type Ca^{2+} channels in neurons heterologously expressing GPR35. The modulation was PTX sensitive, suggesting coupling of GPR35 to the endogenous $G_{i/o}$ protein. We also observed tonic activity of GPR35 which was blocked by PTX treatment. Although there was a population of GPR35b-expressing neurons that did not respond to ligand application, GPR35a and GPR35b displayed no apparent difference in receptor expression pattern.

Materials and Methods

Cloning of GPR35a and GPR35b. GPR35a was amplified from human genomic DNA using the PCR and *PfuUltra* DNA polymerase (Stratagene, La Jolla, CA). Oligonucleotide primers were designed based on AF089087 (GenBank accession number) for subcloning into the mammalian expression vector pCI (Promega, Madison, WI) as follows: forward (*MluI* site underlined) 5'-GATCACGCGTACCATGAATGGCACCTACAACACCTG-3', reverse (*NotI* site underlined) 5'-GATCGCGGCCGCTTAGGCGAGGGTCACGCACAGAG-3'. Fluorescent protein fusion constructs were made in the plasmid Venus-N1 which contains a variant of the yellow fluorescent protein (Nagai et al., 2002). Venus-N1 and was constructed from YFP-N1 (Clontech Laboratories, Mountain View, CA) using QuikChange® Multi (Stratagene) site-directed mutagenesis. For subcloning as a fusion protein into Venus-N1 the following primers were used: forward (*BglII* site underlined) 5'-GATCAGATCTACCATGAATGGCACCT-ACAACACCTG-3', reverse (*HindIII* site underlined) 5'-GATCAAGCTTGGCGAGGGTCAC-GCACAGAG-3'. The blunt PCR products were subcloned into the vector pCRBluntII TOPO (Invitrogen, Carlsbad, CA) for DNA sequencing. Two GPR35a clones were identified: 1) a sequence identical with GenBank accession number AF089087, and 2) an A880C substitution

(referenced to open reading frame) corresponding to a non-synonymous single nucleotide polymorphism (S to R at residue 294). The latter variant has been reported in mRNA sequences CR541765, BC117453 and BC117455. The R294 variant was the first one cloned into the vectors pCI and Venus-N1. Consequently, the S294 version was generated by QuikChange® site directed mutagenesis (Stratagene) from the R294 parent construct.

GPR35b was amplified by the PCR from human whole brain cDNA (Clontech) using *PfuUltra* polymerase. N-terminal primers were derived from the protein sequence of Okumura et al. (2004) and human genomic sequence AF158748: pCI forward (*MluI* site underlined) 5'-GAT-CACGCGTACCATGCTGAGTGGTTCCCGGGCTGTC-3', Venus-N1 forward (*BglII* site underlined) 5'-GATCAGATCTACCATGCTGAGTGGTTCCCGGGCTGTC-3'. C-terminal primers were those used above for GPR35a. The PCR products were subcloned into the vectors pCI and Venus-N1 as above. Sequencing revealed that both GPR35b clones coded for R324 at the residue cognate to position 294 of GPR35a. All constructs were fully sequenced using a CEQ 8000 Automated DNA Sequencer (Beckman-Coulter, Fullerton, CA). Hereafter, the cDNAs cloned into pCI are denoted GPR35a(S294) and GPR35b. The fluorescent protein fusion constructs cloned into Venus-N1 constructs are denoted as GPR35a(S294)-Venus, GPR35a(R294)-Venus, and GPR35b-Venus, respectively.

Isolation of rat SCG neuron and microinjection of cDNA. The protocols for dissociation of rat superior cervical ganglion (SCG) neurons and intranuclear injection of cDNAs have been described in detail previously (Ikeda, 2004; Ikeda and Jeong, 2004). Briefly, adult male Wistar rats were anesthetized with CO_2 inhalation and then decapitated (as approved by the Institutional Animal Care and Use Committee). SCG were isolated from adjacent connective tissues, minced, and put into a flask containing 6 ml of modified Earle's balanced salt solution with enzymes (0.7

mg/ml collagenase D, 0.3 mg/ml trypsin, and 0.05 mg/ml DNase I). The flask with SCG fragments was then shaken at 36 °C for 1 hr. The neurons were subsequently dissociated by shaking the flask forcefully for approximately 15 times, washed, and re-suspended in Minimum Essential Medium (MEM) containing 10% fetal calf serum, 100 U/ml penicillin and 100 µg/ml streptomycin, plated onto poly-L-lysine-coated tissue culture dishes and placed in a 5% CO_2/95% air incubator at 37 °C.

All cDNA constructs were stored at –20 °C as ~1 µg/µl stock solution in TE buffer (10 mM Tris, 1 mM EDTA, pH 8). A FemtoJet 5247 microinjection unit and 5171 micromanipulator (Eppendorf, Madison, WI) were used to inject DNA at a pipette concentration of 200 ng/µl. In some experiments, pEGFP vector plasmid DNA was co-injected at a concentration of 50 ng/µl to aid in identifying successfully injected neurons.

Cell culture, transfection and imaging. HeLa cells were cultured in modified MEM and transfected with cDNAs using fully deacylated polyethylenimine (PEI; Thomas et al., 2005). A mixture of 1 µg of GPR35a(S294)-Venus and 4 µl of PEI at 7.5 mM, or a mixture of 1 µg of GPR35b-Venus and 4 µl of PEI at 7.5 mM was added to 150 µl of Opti-MEM and incubated for 20 min at room temperature. The transfectant mixture was then added to the cell culture dishes.

The transfected HeLa cells were imaged using a 60x 1.4 NA oil-immersion objective mounted on a Nikon inverted fluorescence microscope, a 12-bit cooled CCD camera (Orca-ER, Hamamatsu, Japan) and Volocity 4 software (Improvision Inc., Lexington, MA). SCG neurons were imaged with an Achroplan IR 63x 0.90 NA water-immersion objective mounted on an Zeiss Axioplan 2 microscope (Carl Zeiss, Jena, Germany). The microscope was equipped with a Ti-Sapphire laser (Chameleon, Coherent, Santa Clara, CA) for two-photon imaging. Zeiss software release 3.2 was used for image acquisition.

JPET Fast Forward. Published on October 16, 2007 as DOI: 10.1124/jpet.107.127266
This article has not been copyedited and formatted. The final version may differ from this version.

Ca^{2+} current recordings. Whole cell Ca^{2+} channel currents (I_{Ca}) were recorded from rat SCG neurons using the patch-clamp technique as previously described (Guo and Ikeda, 2005). Custom designed software (S5) was used for generating voltage protocols. Traces were digitized and stimuli delivered with an ITC-18 data acquisition interface (InstruTECH, Port Washington, NY). I_{Ca} traces were filtered at 2 kHz (-3 dB, 4-pole Bessel) and digitized at 10 kHz. A double pulse protocol consisting of two 25 ms test pulses to +10 mV separated by a 50 ms conditioning pulse to +80 mV (Elmslie et al., 1990) was used to evoke I_{Ca}. All recordings were performed at room temperature (22–25 °C).

Solutions and chemicals. The external recording solution contained (in mM): 140 methanesulphonic acid, 145 tetraethylammonium hydroxide (TEA-OH), 10 HEPES, 10 glucose, 10 $CaCl_2$; and 0.0003 tetrodotoxin, pH 7.4 with TEA-OH. The internal solution contained (in mM): 120 N-methyl-D-glucamine, 20 TEA-OH, 11 EGTA, 10 HEPES, 10 sucrose, 10 HCl, 1 $CaCl_2$, 4 MgATP, 0.3 Na_2GTP and 14 Tris creatine phosphate, pH 7.2 with methanesulphonic acid. The osmolalities of the bath and pipette solutions were adjusted with sucrose to 325 and 300 mosmol/kg, respectively. Both KYNA (Tocris, Ellisville, MO) and zaprinast (Sigma-Aldrich, St. Louis, MO) were freshly prepared before experiments. The KYNA stock solution (1 mM in external recording solution) was sonicated to aid dissolution. Zaprinast was dissolved in dimethylsulfoxide (Sigma-Aldrich) at a concentration of 10 mM. Both drugs were then diluted to the final concentration with external recording solution. PTX (List Biological Laboratories Inc., Campbell, CA) was prepared in H_2O at a concentration of 100 µg/ml. MEM, Opti-MEM, penicillin, streptomycin were purchased from Invitrogen, collagenase D from Roche Applied Science (Indianapolis, IN), trypsin (type TRL) from Worthington Biochemical Corporation (Freehold, NJ), and DNase I from Sigma-Aldrich.

JPET Fast Forward. Published on October 16, 2007 as DOI: 10.1124/jpet.107.127266
This article has not been copyedited and formatted. The final version may differ from this version.

Data analyses and statistics. Igor Pro software (WaveMetrics, Lake Oswego, OR) was used to analyze I_{Ca}. The data are presented as mean ± SEM with *n* representing the number of cell tested. The percentage of I_{Ca} inhibition (%) was calculated as $(I_1 - I_2)/I_1$ x 100, where I_1 and I_2 were the prepulse I_{Ca} in the absence or presence of drug application. The prepulse and postpulse I_{Ca} were measured 10 ms after initiation of the test pulse (+10 mV). Facilitation ratio was determined as the ratio of postpulse to prepulse I_{Ca} in the absence or presence of drug application. The concentration-response curves were fit with a Hill equation: $I = I_{max}/\{1 + (EC_{50}/[\text{agonist}])^c\}$, where I, I_{max}, EC_{50}, [agonist] and c are % inhibition, maximum inhibition, concentration producing half maximum response, agonist concentration and Hill coefficient, respectively. Prism 4 software (GraphPad Software, San Diego, CA) was used for statistical comparisons determined by the unpaired *t*-test, one-way ANOVA followed by Newman-Keuls test, repeated measures ANOVA, or Pearson correlation, as noted. $P < 0.05$ was regarded as significant.

Results

Kynurenic acid-induced I_{Ca} inhibition via GPR35a activation. To examine the coupling of GPR35a with endogenous G proteins and effectors, we used sympathetic neurons as surrogate hosts for heterologous expression. We first examined the effect of KYNA application on I_{Ca} recorded from uninjected SCG neurons (Fig. 1A) to establish whether the preparation possessed a suitable null background. I_{Ca} was evoked at 0.1 Hz using a double-pulse voltage protocol (Fig. 1A, left) in solutions designed to isolate I_{Ca}. Under these conditions, the major component of current (65–90%) originated from ω-conotoxin GVIA–sensitive N-type Ca^{2+} channels ($Ca_V2.2$; Ikeda, 1991; Zhu and Ikeda, 1994). The facilitation ratio (Fig. 1, open squares), defined as the ratio of I_{Ca} evoked in the second test pulse (postpulse, Fig. 1, open circles) to first test pulse

JPET Fast Forward. Published on October 16, 2007 as DOI: 10.1124/jpet.107.127266
This article has not been copyedited and formatted. The final version may differ from this version.

(prepulse, Fig. 1, closed circles) was used as a measure of Gβγ–mediated I_{Ca} modulation (Ikeda, 1991; Ikeda, 1996). Basal facilitation ratio (BFR), i.e., facilitation ratio in the absence of drug application, was 1.23 ± 0.03 (n = 4). Application of KYNA (300 μM) for 30 s (Fig. 1A, right) did not alter I_{Ca} (Fig. 1A,D) indicating a lack of functional native GPR35 expression in SCG neurons. Likewise, application of KYNA (300 μM) to SCG neurons expressing EGPF produced no significant I_{Ca} inhibition (0.1 ± 0.8%, n = 4). In contrast, I_{Ca} recorded from a neuron previously injected (approximately 18–24 h) with GPR35a(S294) cDNA (Fig. 2B, left) displayed two characteristic properties of voltage-dependent I_{Ca} inhibition mediated via Gβγ subunit: 1) slowed activation in the prepulse; 2) partial relief of inhibition by a depolarization conditioning pulse (Ikeda, 1996; Herlitze et al., 1996; Ikeda and Dunlap, 1999) as shown by an increase in the facilitation ratio (Fig. 1B, open squares). In the presence of KYNA (300 μM), mean I_{Ca} was inhibited by 38 ± 6% (n = 6, Fig. 1D, hatched bar) and the mean facilitation ratio was increased from 1.44 ± 0.09 to 2.11 ± 0.29 (n = 6). Figure 1B (right) illustrates the time course of KYNA-induced I_{Ca} inhibition. Like other lipid soluble compounds (Guo and Ikeda, 2004), KYNA produced a slowly developing inhibition requiring approximately 60 s to reach a steady-state that slowly recovered following removal of the drug (neurons were superfused with recording solution prior to, during, and after drug application). The kinetics of changes in facilitation ratio are also evident in Figure 1B (right, open squares). To provide a visual indicator for GPR35a(S294) expression, the C-terminus of the receptor was tagged with a fluorescent protein, Venus, an improved variant of EYFP (Nagai et al., 2002). Since the C-terminus of many GPCRs is crucial for receptor trafficking and signal transduction, we tested whether fusion of the fluorescent protein affected the function of GPR35a(S294). Results obtained following expression of GPR35a(S294)-Venus were similar to those illustrated in Fig. 1B. The mean I_{Ca}

JPET Fast Forward. Published on October 16, 2007 as DOI: 10.1124/jpet.107.127266
This article has not been copyedited and formatted. The final version may differ from this version.

inhibition was 51± 5% (n = 5)—a value not significantly different from the inhibition obtained with GPR35a(S294) expression (Fig. 1D, cross hatched bar). When examined with fluorescence microscopy, neurons injected with GPR35a(S294)-Venus cDNA displayed a granular fluorescence pattern and nuclear exclusion (shown later).

Three single nucleotide polymorphism of GPR35a have been previously reported (Horikawa et al., 2000). During generation of the cDNA clones, we identified a non-synonymous substitution, A880C, which codes for the R294 isoform of GPR35a. To examine the function of GPR35a(R294), SCG neurons were injected with a GPR35a(R294)-Venus fusion construct. Figure 1C shows that application of KYNA (300 μM) produced voltage-dependent I_{Ca} modulation similar to that observed in GPR35a(S294) expressing neurons. Average I_{Ca} inhibition in GPR35(R)a-Venus expressing neurons was 36 ± 4% (n = 5. Fig. 1D, solid bar).

Zaprinast-induced I_{Ca} modulation via GPR35a activation. In addition to KYNA, zaprinast, a synthetic phosphodiesterase inhibitor, has been identified as a putative agonist for GPR35 (Taniguchi et al., 2006). Using the strategy employed in Fig. 1, we examined the effects of zaprinast application on I_{Ca} modulation. Zaprinast (10 μM) did not affect mean I_{Ca} inhibition in uninjected neurons (2 ± 1%, n = 4; Fig 2B, open bar) or neurons expressing EGFP (0.6 ± 1.2%, n = 4) providing additional evidence for a lack of functional GPR35 expression in SCG neurons. Like KYNA, application of zaprinast (10 μM) resulted in I_{Ca} inhibition in GPR35a(S294)-expressing neurons. Zaprinast-induced I_{Ca} modulation was also voltage-dependent based on the slowing of activation (Fig. 2A, left) and increased facilitation ratio (from 1.52 ± 0.09 to 2.88 ± 0.46, n = 4; Fig. 2A. right, open squares). Figure 2A (right) depicts the time course of zaprinast-induced I_{Ca} inhibition which was relatively slow in onset usually taking about 60 s to reach a steady-state. The washout of zaprinast was even slower taking several minutes to

JPET Fast Forward. Published on October 16, 2007 as DOI: 10.1124/jpet.107.127266
This article has not been copyedited and formatted. The final version may differ from this version.

complete. Mean I_{Ca} inhibition produced by 10 μM zaprinast was 59 ± 8 (n = 4), 55 ± 4 (n = 4), 42 ± 4% (n = 4) for neurons injected with GPR35a(S294), GPR35a(S294)-Venus, or GPR35a(R294)-Venus cDNAs, respectively (Fig. 2B). There was no significant difference among zaprinast-induced mean I_{Ca} inhibition in the three constructs ($P > 0.05$; ANOVA).

Concentration-dependence of KYNA- and zaprinast-mediated I_{Ca} inhibition. Figure 2C illustrates the concentration-response curves for I_{Ca} inhibition generated from GPR35a(S294)-Venus expressing SCG neurons. Because of the slow drug washout, only a single concentration of agonist was applied to each neuron. The data points represent the mean inhibition (%) calculated from 2–8 cells (as labeled) for either KYNA (filled circles) or zaprinast (open circles). These data were fit with a Hill equation using a nonlinear least squares algorithm. From these analyses, the maximum inhibitions, EC_{50} values, and Hill coefficients were 56 and 59%, 58 and 1.1 μM, 1.1 and 1.6, for KYNA and zaprinast, respectively. The data indicate that zaprinast was more potent than KYNA but had a similar efficacy.

Signaling pathways mediating I_{Ca} inhibition. A hallmark of I_{Ca} inhibition mediated by the Gβγ arm of the heterotrimeric G-protein pathway is voltage-dependence. At depolarized membrane potentials, the affinity of the channel for Gβγ is believed to decrease thereby relieving I_{Ca} inhibition. Both the agonist-mediated slowing of current activation and increase in facilitation ratio shown previously (Figs. 1,2) are indicative of voltage-dependent Gβγ-mediated signaling (Ikeda and Dunlap, 1999). To examine the voltage-dependence of GPR35a-mediated I_{Ca} modulation in greater detail, current-voltage (I-V) relationships in the absence or presence of KYNA were generated by evoking families of I_{Ca} with 70 ms test pulses over the range -120 to +80 mV from a holding potential of -80 mV. Figure 3A illustrates normalized mean I-V curves obtained in the absence (open circles) or presence of KYNA (filled circles). I_{Ca} amplitude was

normalized to the maximal I_{Ca} amplitude which usually occurred at step potential near +5 mV in the absence of KYNA. I_{Ca} inhibition appears most prominent at membrane potentials generating the largest I_{Ca} amplitude. To quantify this impression, I_{Ca} inhibition for five individual neurons obtained at test potentials of 0, +20, and +40 mV are plotted in 3B. Although the degree of I_{Ca} inhibition varied for each neuron, the magnitude of inhibition consistently decreased with increasing test potential. Consequently, mean inhibition at each potential was significantly different ($P < 0.001$) as determined by repeated measures ANOVA.

Although voltage-dependence implicates the Gβγ subunit as the mediator of I_{Ca} modulation, the composition of the G-protein heterotrimer, especially the Gα-subunit is important for receptor coupling. Previous studies suggest that the $G_{i/o}$ proteins couple efficiently to GPR35a. Therefore, SCG neurons were pre-treated with PTX (500 ng/ml) for 8–24 hr prior to agonist application and electrophysiological recording. Pretreatment with PTX completely abolished both KYNA (100 μM) and zaprinast (10 μM)-induced I_{Ca} inhibition in GPR35a-expressing neurons (1.9 ± 0.4%, n = 4, 1.4 ± 1%, n = 4, respectively) as illustrated in Fig. 3B. Taken together, these data indicate that Gβγ released from $G\alpha_{i/o}$ containing G-protein heterotrimers mediates I_{Ca} inhibition following agonist binding to GPR35a.

Tonic activity of GPR35a. Although agonist occupancy is usually required for GPCR activation, some GPCRs, such as the CB1 cannabinoid receptor, 5-HT_{2c} serotonin receptor, M_1-M_5 muscarinic acetylcholine receptor, and β2 adrenergic receptor, display tonic activity in the absence of overt ligand (de Ligt et al., 2000). In the course of these studies, we found that the expression of GPR35a significantly increased BFR (Fig. 4A), an indicator of tonic G-protein modulation (Ikeda, 1991). The mean BFR in GPR35a(S294) and GPR35a(S294)-Venus expressing neurons was 1.60 ± 0.12 (n = 13) and 1.50 ± 0.04 (n = 60), respectively, compared

JPET Fast Forward. Published on October 16, 2007 as DOI: 10.1124/jpet.107.127266
This article has not been copyedited and formatted. The final version may differ from this version.

with 1.25 ± 0.03 (n = 24) in control (uninjected) neurons. BFR in GPR35a(R294)-Venus injected neurons was 1.35 ± 0.06 (n = 13), which was not significantly different from that of uninjected neurons. In GPR35a-expressing neurons, there was a significant positive correlation between I_{Ca} inhibition induced by zaprinast or KYNA (both at supramaximal concentrations) and BFR (Pearson correlation coefficient, r = 0.46, P < 0.05; Fig. 4B). As BFR is an indicator of tonic G protein activation, the correlation implies that the tonic activity of GPR35a is related to receptor expression level.

To assess whether the tonic activity of GPR35a required coupling to $G_{i/o}$ proteins, we examined the effect of PTX on BFR in neurons expressing GPR35(S)a-Venus. Mean BFR decreased from 1.52 ± 0.06 (n = 12) to 1.27 ± 0.02 (n = 8) following PTX treatment (Fig. 4C). The mean BFR between uninjected neurons (Fig. 4C, open bar) and PTX treated GPR35(S)a-Venus expressing neurons (Fig. 4C, filled bar) was not significantly different, suggesting that the tonic activity of GPR35 arose from activation of $G_{i/o}$ protein.

GPR35b-mediated I_{Ca} inhibition. In humans, alternative splicing of the GPR35 primary transcript produces both GPR35a and GPR35b mRNA. The latter isoform is predicted to code for an additional 31 additional amino acids at the N-terminus of the receptor (Okumura et al., 2004). As functional studies of GPR35b have not been published, we examined the effects of KYNA and zaprinast application on I_{Ca} modulation in GPR35b-expressing neurons. For GPR35b-injected neurons, two populations emerged based on the response to agonist application. In 4 of 7 cells, zaprinast (10 μM) produced significant I_{Ca} inhibition (> 20 %; Fig. 5A, bottom). Similarly, KYNA (300 μM) inhibited I_{Ca} by more than 20% in 5 of 8 cells (Fig. 5A, top). As in GPR35a-expressing neurons, the GPR35b-mediated I_{Ca} inhibition displayed characteristic voltage-dependent properties. The mean facilitation ratio increased from 1.70 ±

JPET Fast Forward. Published on October 16, 2007 as DOI: 10.1124/jpet.107.127266
This article has not been copyedited and formatted. The final version may differ from this version.

0.10 to 2.87 ± 0.13 in the presence of 10 μM zaprinast (n = 4) and from 1.38 ± 0.08 to 1.97 ± 0.20 in the presence of 300 μM KYNA (n = 5). Comparison of mean agonist-induced (either KYNA or zaprinast) I_{Ca} inhibition for either GPR35a– or GPR35b–expressing neurons revealed similar values when "non-responding" cells were excluded from the analysis (Fig. 5B). To determine whether a fluorescent tag on the C-terminus of GPR35b affected function, we monitored I_{Ca} inhibition in GPR35b-Venus expressing neurons. In these cells, KYNA (300 μM) application produced a typical voltage-dependent I_{Ca} inhibition (data not shown) and there was no significant difference in mean I_{Ca} inhibition between GPR35b (37 ± 6%, n = 5) and GPR35b-Venus (38 ± 3%, n = 5) expressing neurons. Figure 5C illustrates the relationship between mean I_{Ca} inhibition in GPR35b-Venus expressing neurons and KYNA concentration. When responses of less than 20% (shown as open circles) were excluded, the mean data (filled triangles) were well fit (solid line) with a Hill equation with maximum inhibition, EC_{50} , and Hill coefficient of 49%, 66 μM, and 1.0, respectively. As in GPR35a-expressing neurons, agonist (zaprinast or KYNA)-induced I_{Ca} inhibition was significantly correlated to the BFR in GPR35b-expressing neurons (Pearson correlation coefficient, r = 0.70, $p < 0.005$; Fig. 5D).

Subcellular localization of GPR35-Venus fusion proteins. In contrast to GPR35a-mediated I_{Ca} modulation, injection of GPR35b cDNA into neurons produced highly variable responses. We thus examined whether the additional 31 amino acids in the N-terminus of GPR35b affected the trafficking or expression pattern of the receptor. GPR35a (Fig. 6, left) or GPR35b (Fig. 6, right) fused to the fluorescent protein Venus were expressed in HeLa cells (Fig. 6, top row) or SCG neurons (Fig. 6, bottom row). HeLa cells were imaged using conventional wide-field fluorescence microscopy whereas SCG neurons were imaged using two-photon microscopy. In GPR35a/b-expressing HeLa cells, fluorescence appeared in discrete cellular compartments as

well as near (or on) the plasma membrane. The focal plane in these images was near the cell/cover glass interface and shows a similar fluorescence pattern for both GPR35 splice variants. Surprisingly, in the GPR35a/b-expressing SCG neurons fluorescence was found throughout the cytoplasm, was excluded from the nucleus, and showed no obvious enrichment near the plasma membrane ("rim staining") as would be expected (given that both GPR35 constructs were functional). The fluorescence pattern in the cytoplasm was granular and thus different from the even distribution seen when expressing soluble (i.e., non-fusion) fluorescent proteins. Thus, we are limited to the interpretation that the fluorescence patterns of GPR35a and GPR35b were similar and thus the additional residues found in GPR35b did not overtly alter trafficking.

DISCUSSION

In the present study, we demonstrated that GPR35, when heterologously expressed in sympathetic neurons, couples via native heterotrimeric G-proteins to modulate N-type Ca^{2+} channels. Two recently discovered GPR35 agonists, kynurenic acid and zaprinast, activated GPR35 to produce I_{Ca} inhibition that was PTX-sensitive and voltage-dependent. Zaprinast was more potent than kynurenic acid but possessed similar efficacy. In addition, the receptor appeared to activate PTX-sensitive G-protein in the absence of overt agonist. Two isoforms of GPR35a and a splice variant, GPR35b, produced similar effects although variability was greater with the latter. Expression of fluorescent protein fusion constructs of GPR35a and GPR35b revealed similar expression patterns from which limited inference could be drawn.

Although gene analysis studies implicate GPR35 in gastric cancer (Okumura et al., 2004), Albright hereditary osteodystrophy (Shrimpton et al., 2004), and type II diabetes (Vander Molen et al., 2005), basic information regarding the pharmacology, physiology, and function of GPR35

is scarce. In humans, high levels of GPR35 mRNA were detected in the immune and digestive system, including peripheral leukocytes, spleen, small intestine, colon, and stomach with levels reported for brain (O'Dowd et al., 1998; Wang et al., 2006). However, GPR35a cDNA was isolated from a human dorsal root ganglion cDNA (Taniguchi et al., 2006), and in this study, we cloned GPR35b from human whole brain cDNA. In addition, high throughput *in situ* hybridization studies indicate substantial levels of GPR35 mRNA (Lein et al., 2007) throughout the mouse brain. Therefore, there is accumulating evidence for the expression of GPR35 in both the central and peripheral nervous system.

Recently, KYNA (Wang et al., 2006) and zaprinast (Taniguchi et al., 2006) were identified as GPR35 agonists using high throughput screening methods. Kynurenic acid is a tryptophan metabolite in the kyneurenine pathway. Although serotonin and melatonin, two other tryptophan metabolites, are well known ligands for GPCRs, there is limited knowledge about the function of KYNA. In the central nervous system, KYNA is produced by astrocytes and neurons and exerts a neuroprotective effect. Kynurenic acid is a potential endogenous antagonist of NMDA receptors and α7 nicotinic receptors (Stone, 2000; Hilmas et al., 2001) and has a dual action on AMPA receptor (Prescott et al., 2006). At lower KYNA concentrations (nM to μM), AMPA receptor responses are facilitated whereas higher KYNA concentrations (mM) antagonize the receptor. In the present study, we showed that KYNA inhibited neuronal N-type Ca^{2+} channels via activation of heterologously expressed GPR35. Thus, endogenous KYNA may play a role in the regulation of neuronal excitability and synaptic release by acting at GPR35. To our knowledge, this is the first study to examine the effect of KYNA on G-protein mediated Ca^{2+} channel modulation. The concentration of KYNA necessary to activate GPR35 (10 μM – 1 mM) is within the range used to probe ionotropic glutamate receptor function (Prescott et al., 2006).

JPET Fast Forward. Published on October 16, 2007 as DOI: 10.1124/jpet.107.127266
This article has not been copyedited and formatted. The final version may differ from this version.

However, levels of KYNA in extracellular fluid of the rat striatum is around 17 nM (Swartz et al., 1990), approximately three orders of magnitude less than the EC_{50} for GPR35 activation reported here and in a previous study (Wang et al., 2006). Thus, although GPR35 activation should be considered a potential mechanism when interpreting data obtained with KYNA in a similar concentration range, another, as yet unidentified, substance likely serves as the endogenous ligand.

Zaprinast is characterized as a selective cGMP-specific PDE5 inhibitor and, as such, is used as a tool to identify signal transduction pathways incorporating generation/degradation of cGMP (reviewed by Gibson, 2001). Therefore, the discovery that zaprinast serves as a relatively potent GPR35 agonist (Taniguchi et al., 2006) impacts the interpretation of data in which zaprinast was assumed to solely affect cGMP degradation. For example, zaprinast induced a significant depression of basal synaptic transmission in rat hippocampus attributed to elevation of intracellular cGMP level (Monfort et al., 2002; Makhinson et al., 2006). However, our data provide evidence for the *potential* modulation of presynaptic Ca^{2+} channels by zaprinast acting as a GPR35 agonist. It should be noted, however, that the presence of GPR35 in presynaptic terminals and the coupling of natively expressed GPR35 to Ca^{2+} channels have not been established. Although a direct modulation of N-type Ca^{2+} channel by cGMP has been reported (Meriney et al., 1994; Grassi et al., 2004), the zaprinast-induced Ca^{2+} channel inhibition seen here was unlikely due to increased intracellular [cGMP] because: 1) zaprinast had no effect on I_{Ca} in the absence of GPR35 expression, and 2) zaprinast produced I_{Ca} modulation with all the hallmarks of a direct Gβγ effect.

In this study, we also provided evidence that GPR35a and GPR35b were tonically active (i.e., in the absence of overt agonist) when expressed in rat sympathetic neurons (Figs. 4,5). Following

JPET Fast Forward. Published on October 16, 2007 as DOI: 10.1124/jpet.107.127266
This article has not been copyedited and formatted. The final version may differ from this version.

GPR35 expression, the BFR, a sensitive indicator of tonic G-protein activation (Ikeda, 1991), was elevated. This elevation was abolished following PTX treatment implicating the activation of endogenous $G_{i/o}$ proteins. Tonic GPCR activity likely depends on receptor cell surface density (de Ligt et al., 2000; Cotecchia, 2007). For example, increasing the density of β2-adrenergic receptors results in the elevation of basal receptor-mediated generation of cyclic AMP (Chidiac et al., 1994). In this study, there was a positive correlation between BFR and the degree of agonist-induced I_{Ca} inhibition, suggesting that receptor number contributes to the tonic activity of GPR35. In addition, these data suggest that receptor levels required for full agonist efficacy also produce tonic activation. Consequently, tonic GPR35 activity may not require artifactual levels of expression and thus contribute to the function of GPR35 within a physiological context. It should be noted, however, that, in the absence of well-characterized neutral antagonist, one cannot exclude the existence of endogenous agonists. Thus, the interpretation that tonic activity equates to constitutive activity arising from non-ligand bound receptors remains an open question.

At present, there are no studies comparing the coupling of GPR35 isoforms and splice variants to endogenous signaling systems. We examined two isoforms of GPR35a (S294 and R294) and splice variant, GPR35b which contains an additional 31 amino acids at the N-terminus. In general, the biophysical characteristics of I_{Ca} modulation and pharmacological parameters determined following expression of the various GPR35 cDNAs were similar. The only apparent anomaly was an increased response variability following GPR35b expression. Suspecting a potential difference in cellular trafficking between GPR35a and GPR35b, we examined fluorescence protein of fusions of GPR35 expressed in either HeLa cells or SCG neurons. Surprisingly, although the fusion proteins were fully functional in terms of I_{Ca}

JPET Fast Forward. Published on October 16, 2007 as DOI: 10.1124/jpet.107.127266
This article has not been copyedited and formatted. The final version may differ from this version.

inhibition, the vast majority of fluorescence was located in the cytosol (although possibly on internal membranes) of SCG neurons instead of concentrated near the cell surface. Thus, we can infer only that the expression pattern of GPR35a and GPR35b were superficially similar and thus the mechanism underlying the variability in GPR35b responses remains unclear.

Taken together, the present study demonstrates the coupling of GPR35 to endogenous G-proteins that modulate neuronal Ca^{2+} channel and thereby provides evidence for a potential role of GPR35 in regulating neuronal excitability and synaptic transmission.

Acknowledgements

We thank Dr. Steven S. Vogel for assisting with two-photon confocal imaging.

References

Baker D, Pryce G, Davies WL, and Hiley CR (2006) *In silico* patent searching reveals a new cannabinoid receptor. *Trends Pharmacol Sci* **27**:1–4.

Chidiac P, Hebert TE, Valiquette M, Dennis M, and Bouvier M (1994) Inverse agonist activity of β-adrenergic antagonists. *Mol Pharmacol* **45**:490–499.

Cotecchia S (2007) Constitutive activity and inverse agonism at the α1 adrenoceptors. *Biochem Pharmacol* **73**:1076–1003.

de Ligt RA, Kourounakis AP, and IJzerman AP (2000). Inverse agonism at G protein-coupled receptors: (patho)physiological relevance and implications for drug discovery. *Br J Pharmacol* **130**:1–12.

Elmslie KS, Zhou W, and Jones SW (1990) LHRH and GTP-γ-S modify calcium current activation in bullfrog sympathetic neurons. *Neuron* **5**:75–80.

Gibson A (2001) Phosphodiesterase 5 inhibitors and nitrergic transmission - from zaprinast to sildenafil. *Eur J Pharmacol* **411**:1–10.

Grassi C, D'Ascenzo M, and Azzena GB (2004) Modulation of $Ca_v2.1$ and $Ca_v2.2$ channels induced by nitric oxide via cGMP-dependent protein kinase. *Neurochem Int* **45**:885–893.

Guo J and Ikeda SR (2005) Coupling of metabotropic glutamate receptor 8 to N-type Ca^{2+} channels in rat sympathetic neurons. *Mol Pharmacol* **67**:1840–1851.

Guo J and Ikeda SR (2004) Endocannabinoids modulate N-type calcium channels and G-protein-coupled inwardly rectifying potassium channels via CB1 cannabinoid receptors heterologously expressed in mammalian neurons. *Mol Pharmacol* **65**:665–674.

Herlitze S, Garcia DE, Mackie K, Hille B, Scheuer T, and Catterall WA (1996) Modulation of Ca^{2+} channels by G-protein βγ subunits. *Nature* **380**:258–262.

Hilmas C, Pereira EF, Alkondon M, Rassoulpour A, Schwarcz R, and Albuquerque EX (2001) The brain metabolite kynurenic acid inhibits α7 nicotinic receptor activity and increases non-α7 nicotinic receptor expression: physiopathological implications. *J Neurosci* **21**:7463–7473.

Horikawa Y, Oda N, Cox NJ, Li X, Orho-Melander M, Hara M, Hinokio Y, Lindner TH, Mashima H, Schwarz PE, del Bosque-Plata L, Horikawa Y, Oda Y, Yoshiuchi I, Colilla S, Polonsky KS, Wei S, Concannon P, Iwasaki N, Schulze J, Baier LJ, Bogardus C, Groop L, Boerwinkle E, Hanis CL, and Bell GI (2000) Genetic variation in the gene encoding calpain-10 is associated with type 2 diabetes mellitus. *Nat Genet* **26**:163–175.

Ikeda SR (1991) Double-pulse calcium channel current facilitation in adult rat sympathetic neurones. *J Physiol* **439**:181–214.

Ikeda SR (1996) Voltage-dependent modulation of N-type calcium channels by G-protein βγ subunits. *Nature* **380**:255–258.

Ikeda SR (2004) Expression of G-protein signaling components in adult mammalian neurons by microinjection. *Methods Mol Biol* **259**:167–181.

Ikeda SR and Dunlap K (1999) Voltage-dependent modulation of N-type calcium channels: role of G protein subunits. *Adv Second Messenger Phosphoprotein Res* **33**: 131–151.

Ikeda SR and Jeong SW (2004) Use of RGS-insensitive Gα subunits to study endogenous RGS protein action on G-protein modulation of N-type calcium channels in sympathetic neurons. *Methods Enzymol* **389**:170–189.

Kostenis E, Waelbroeck M, and Milligan G (2005) Techniques: promiscuous Galpha proteins in basic research and drug discovery. *Trends Pharmacol Sci* **26**:595–602.

Lein ES, Hawrylycz MJ, Ao N, Ayres M, Bensinger A, Bernard A, Boe AF, Boguski MS, Brockway KS, Byrnes EJ, Chen L, Chen L, Chen TM, Chin MC, Chong J, Crook BE, Czaplinska A, Dang CN, Datta S, Dee NR, Desaki AL, Desta T, Diep E, Dolbeare TA, Donelan MJ, Dong HW, Dougherty JG, Duncan BJ, Ebbert AJ, Eichele G, Estin LK, Faber C, Facer BA, Fields R, Fischer SR, Fliss TP, Frensley C, Gates SN, Glattfelder KJ, Halverson KR, Hart MR, Hohmann JG, Howell MP, Jeung DP, Johnson RA, Karr PT, Kawal R, Kidney JM, Knapik RH, Kuan CL, Lake JH, Laramee AR, Larsen KD, Lau C, Lemon TA, Liang AJ, Liu Y, Luong LT, Michaels J, Morgan JJ, Morgan RJ, Mortrud MT, Mosqueda NF, Ng LL, Ng R, Orta GJ, Overly CC, Pak TH, Parry SE, Pathak SD, Pearson OC, Puchalski RB, Riley ZL, Rockett HR, Rowland SA, Royall JJ, Ruiz MJ, Sarno NR, Schaffnit K, Shapovalova NV, Sivisay T, Slaughterbeck CR, Smith SC, Smith KA, Smith BI, Sodt AJ, Stewart NN, Stumpf KR, Sunkin SM, Sutram M, Tam A, Teemer CD, Thaller C, Thompson CL, Varnam LR, Visel A, Whitlock RM, Wohnoutka PE, Wolkey CK, Wong VY, Wood M, Yaylaoglu MB, Young RC, Youngstrom BL, Yuan XF, Zhang B, Zwingman TA, and Jones AR. (2007) Genome-wide atlas of gene expression in the adult mouse brain. *Nature* **445**:168–176.

Makhinson M, Opazo P, Carlisle HJ, Godsil B, Grant SG, and O'Dell TJ (2006). A novel role for cyclic guanosine 3',5'monophosphate signaling in synaptic plasticity: a selective suppressor of protein kinase A-dependent forms of long-term potentiation. *Neuroscience* **140**:415–431.

Meriney SD, Gray DB, and Pilar GR (1994) Somatostatin-induced inhibition of neuronal Ca^{2+} current modulated by cGMP-dependent protein kinase. *Nature* **369**:336–339.

Milman G, Maor Y, Abu-Lafi S, Horowitz M, Gallily R, Batkai S, Mo FM, Offertaler L, Pacher P, Kunos G, Mechoulam R (2006) N-arachidonoyl L-serine, an endocannabinoid-like brain constituent with vasodilatory properties. *Proc Natl Acad Sci USA.* **103**:2428–2433.

Monfort P, Munoz MD, Kosenko E, and Felipo V (2002) Long-term potentiation in hippocampus involves sequential activation of soluble guanylate cyclase, cGMP-dependent protein kinase, and cGMP-degrading phosphodiesterase. *J Neurosci* **22**:10116–10122.

Nagai T, Ibata K, Park ES, Kubota M, Mikoshiba K, and Miyawaki A (2002) A variant of yellow fluorescent protein with fast and efficient maturation for cell-biological applications. *Nat Biotechnol* **20**:87–90.

O'Dowd BF, Nguyen T, Marchese A, Cheng R, Lynch KR, Heng HH, Kolakowski LF Jr, and George SR (1998) Discovery of three novel G-protein-coupled receptor genes. *Genomics* **47**:310–313.

Okumura S, Baba H, Kumada T, Nanmoku K, Nakajima H, Nakane Y, Hioki K, Ikenaka K (2004) Cloning of a G-protein-coupled receptor that shows an activity to transform NIH3T3 cells and is expressed in gastric cancer cells. *Cancer Sci* **95**:131–135.

Petitet F, Donlan M, and Michel A (2006) GPR55 as a new cannabinoid receptor: still a long way to prove it. *Chem Biol Drug Des* **67**:252–253.

Prescott C, Weeks AM, Staley KJ, and Partin KM (2006) Kynurenic acid has a dual action on AMPA receptor responses. *Neurosci Lett* **402**:108–112.

Shrimpton AE, Braddock BR, Thomson LL, Stein CK, and Hoo JJ (2004) Molecular delineation of deletions on 2q37.3 in three cases with an Albright hereditary osteodystrophy-like phenotype. *Clin Genet* **66**:537–544.

Stadel JM, Wilson S, and Bergsma, DJ (1997) Orphan G protein-coupled receptors: a neglected opportunity for pioneer drug discovery. *Trends Pharmacol Sci* **18**:430–437.

Stone TW (2000) Development and therapeutic potential of kynurenic acid and kynurenine derivatives for neuroprotection. *Trends Pharmacol Sci* **21**:149–154.

Swartz KJ, During MJ, Freese A, and Beal, MF (1990) Cerebral synthesis and release of kynurenic acid: an endogenous antagonists of excitatory amino acid receptors. *J Neurosci* **10**:2965–2973.

Taniguchi Y, Tonai-Kachi H, and Shinjo K (2006) Zaprinast, a well-known cyclic guanosine monophosphate-specific phosphodiesterase inhibitor, is an agonist for GPR35. *FEBS Lett* **580**: 5003–5008.

Thomas M, Lu JJ, Ge Q, Zhang C, Chen J, and Klibanov AM (2005) Full deacylation of polyethylenimine dramatically boosts its gene delivery efficiency and specificity to mouse lung. *Proc Natl Acad Sci USA* **102**:5679–5684.

Vander Molen J, Frisse LM, Fullerton SM, Qian Y, del Bosque-Plata L, Hudson RR, and Di Rienzo A (2005). Population genetics of CAPN10 and GPR35: implications for the evolution of type 2 diabetes variants. *Am J Hum Genet* **76**:548–60.

Wang J, Simonavicius N, Wu X, Swaminath G, Reagan J, Tian H, and Ling L (2006) Kynurenic acid as a ligand for orphan G protein-coupled receptor GPR35. *J Biol Chem* **281**:22021–22028.

Zhu Y and Ikeda, SR (1994) VIP inhibits N-type Ca^{2+} channels of sympathetic neurons via a pertussis toxin-insensitive but cholera toxin-sensitive pathway. *Neuron* **13**:657–669.

Footnotes

This work was supported by the intramural program of the National Institutes of Health, National Institute on Alcohol Abuse and Alcoholism, Bethesda, MD 20892.

JPET Fast Forward. Published on October 16, 2007 as DOI: 10.1124/jpet.107.127266
This article has not been copyedited and formatted. The final version may differ from this version.

Legends for Figures

Fig. 1. Kynurenic acid (KYNA) mediated inhibition of N-type ($Ca_V2.2$) Ca^{2+} channel currents (I_{Ca}) in rat SCG neurons heterologously expressing GPR35a. **A**, representative traces of whole-cell I_{Ca} (left panel) evoked with a double-pulse voltage protocol (bottom) prior to (control) or during application of KYNA (300 μM) recorded from an uninjected (control) neuron. The dashed line represents the zero current level. The time course of prepulse I_{Ca} amplitude (filled circles), postpulse I_{Ca} amplitude (open circles), and facilitation ratio (postpulse/prepulse amplitude, open squares) during agonist application (solid bar) is illustrated in the right panel. I_{Ca} amplitude was measured at 10 ms following initiation of the +10 mV test pulse. **B**, **C** I_{Ca} traces (left panel) and time courses (right panel) for a neuron previously injected with GPR35a(S294) or GPR35a(R294)-Venus cDNA. Injected cells were identified from fluorescence emanating from a fluorescent protein (B) expressed from a co-injected plasmid (pEGPF-N1) or directly from the fluorescent protein fusion (C). **D**, mean ± SEM prepulse I_{Ca} inhibition produced following application of KYNA (300 μM) to neurons previously injected with cDNA coding for the GPR35a isoform indicated below the bar. The numbers of cells tested are listed in parentheses.

Fig. 2. Zaprinast mediated inhibition of I_{Ca} in GPR35a expressing neurons. **A**, superimposed I_{Ca} traces (left) and time courses (right panel) recorded from neurons expressing GPR35a(S294) in either the absence or presence of zaprinast (10 μM). **B**, mean ± SEM prepulse I_{Ca} inhibition produced following application of zaprinast (10 μM) to neurons previously injected with cDNA coding for the GPR35a isoform indicated below the bar. **C**, concentration-response plot for KYNA (filled circles) or zaprinast (open circles) mediated I_{Ca} inhibition in GPR35a(S294)-

JPET Fast Forward. Published on October 16, 2007 as DOI: 10.1124/jpet.107.127266
This article has not been copyedited and formatted. The final version may differ from this version.

Venus expressing neurons. Mean ± SEM data were fit with a Hill equation (solid line) using a nonlinear least squares algorithm. Numbers in parentheses indicate the number of cell tested.

Fig. 3. Characteristics of GPR35a-mediated I_{Ca} inhibition. **A**, normalized current-voltage (*I-V*) relationships (left panel) generated in the absence (open circles) or presence (filled circles) of KYNA (100 μM). Ca^{2+} currents were elicited from a holding potential of -80 mV with 70 ms voltage steps over the range -120 to +80 mV. I_{Ca} at each test pulse was normalized to the I_{Ca} elicited by the depolarizing step to +5 mV in the absence of KYNA. The percentage I_{Ca} inhibition produced by KYNA (100 μM) at three membrane potentials (right panel) for five neurons. Mean inhibition at each potential was significantly different ($P < 0.001$) as determined by repeated measures ANOVA. **B**, superimposed I_{Ca} traces (left) recorded in the absence or presence of 100 μM KYNA (*top*) or 10 μM zaprinast (bottom) from GPR35a-expressing neurons pretreated 8–24 hrs earlier with *Bordetalla pertussis* toxin (PTX). Bar graph (right panel) of mean ± SEM I_{Ca} inhibition produced by KYNA or zaprinast in GPR35a-expressing control neurons (filled bars) neurons pretreated with PTX (open bars). Numbers in parentheses indicate the number of cell tested.

Fig. 4. Expression of GPR35a results in tonic G-protein activation. **A**, bar graph of mean ± SEM basal facilitation ratio (BFR) from control neurons (open) or neurons expressing GPR35a(S294) (hatched), GPR35a(S294)-Venus (cross hatched), or GPR35a(R294)-Venus (filled). BFR is the ratio of postpulse/prepulse I_{Ca} amplitude in the absence of agonist. Means were compared using one-way ANOVA and Neuman-Keuls post hoc analysis. **B**, plot of I_{Ca} inhibition for individual GPR35a-expressing neurons versus the BFR. Data were analyzed using Pearson's correlation. **C**,

JPET Fast Forward. Published on October 16, 2007 as DOI: 10.1124/jpet.107.127266
This article has not been copyedited and formatted. The final version may differ from this version.

bar graph of mean ± SEM BFR from neurons expressing GPR35a(S294)-Venus either without (open) or with pretreatment with PTX (filled). Means were compared with a non-paired Student's t-test. Numbers in parentheses indicate the number of neuron tested. * indicates $P < 0.05$.

Fig. 5. Agonist-induced I_{Ca} inhibition in rat SCG neurons expressing GPR35b. **A**, superimposed I_{Ca} traces recorded with the double-pulse voltage protocol from GPR35b expressing neurons in the absence or presence of KYNA (300 μM, top traces) or zaprinast (10 μM, bottom traces). **B**, summary bar graph of mean ± SEM I_{Ca} inhibition produced by KYNA (left) or zaprinast (right) from neurons expressing GPR35a(S294) (open) or GPR35b (filled). **C,** concentration-response for KYNA-induced I_{Ca} inhibition in GPR35b-Venus expressing neurons. The open circles represent the cells excluded from the analysis. Filled triangles represent mean ± SEM for the numbers of neurons indicated in parentheses. Solid line represents the best fit to a Hill equation generated as in Fig. 2C. **D**, I_{Ca} inhibition plotted versus the BFR for individual GPR35b-expressing neurons. Data were analyzed using Pearson's correlation.

Fig. 6. Expression of GPR35 fluorescent protein fusion constructs in HeLa cells and rat sympathetic neurons. Fluorescence images of HeLa cells expressing GPR35a(S294)-Venus (*top left*) and GPR35b-Venus (*top right*). Cells were imaged using conventional wide-field fluorescence microscopy. Fluorescence images of SCG neurons expressing GPR35a(S294)-Venus (*bottom left*) and GPR35b-Venus (*bottom right*). Neurons were imaged using two-photon confocal microscopy. Horizontal scale bars represent 10 μm.

Figure 1

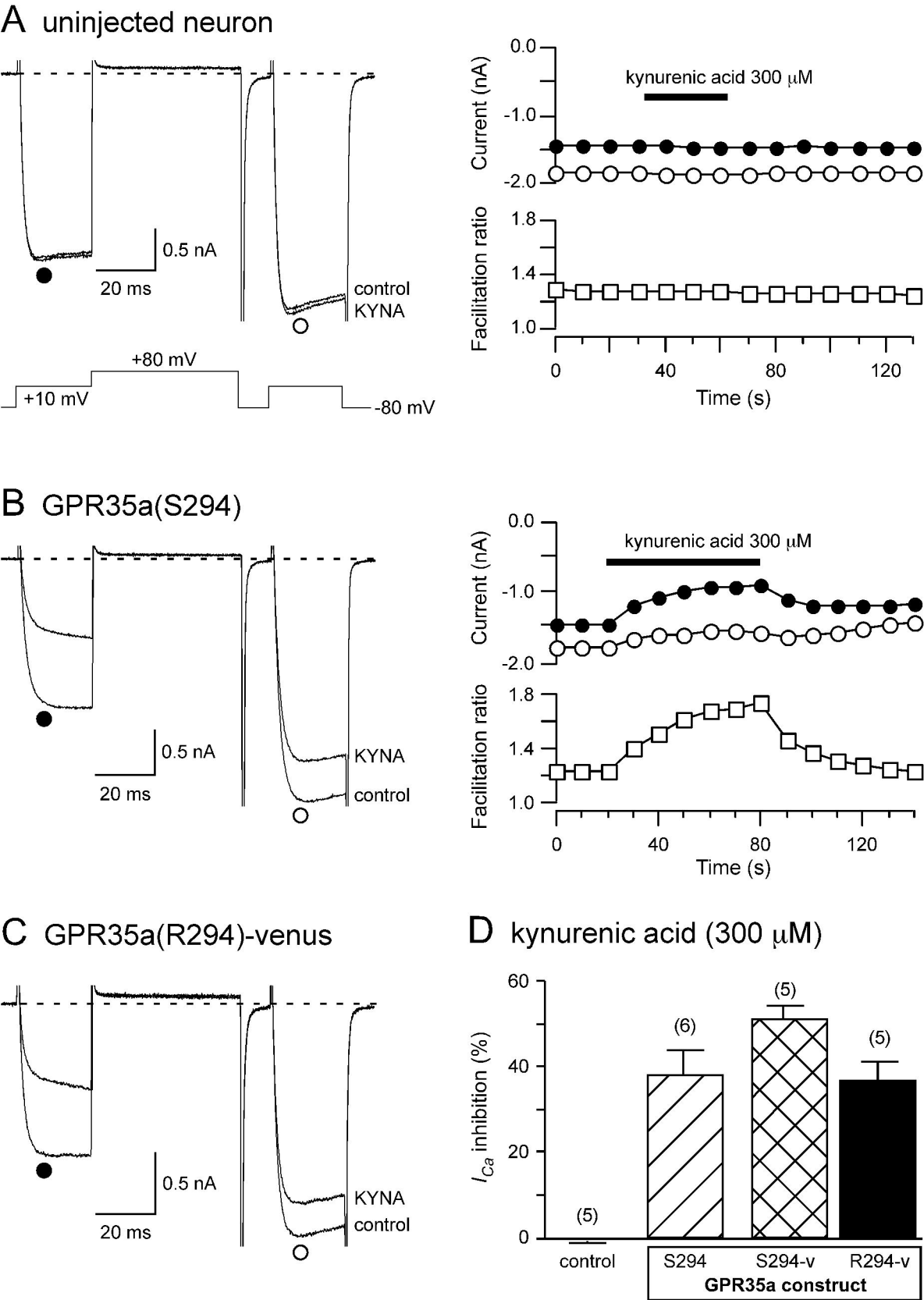
A uninjected neuron
0.5 nA
20 ms
control
KYNA
+80 mV
+10 mV
-80 mV
kynurenic acid 300 μM
Current (nA)
0.0
-1.0
-2.0
Facilitation ratio
1.8
1.4
1.0
0
40
80
120
Time (s)
B GPR35a(S294)
0.5 nA
20 ms
KYNA
control
kynurenic acid 300 μM
Current (nA)
0.0
-1.0
-2.0
Facilitation ratio
1.8
1.4
1.0
0
40
80
120
Time (s)
C GPR35a(R294)-venus
0.5 nA
20 ms
KYNA
control
D kynurenic acid (300 μM)
I_{Ca} inhibition (%)
60
40
20
0
(5)
(6)
(5)
(5)
control
S294
S294-v
R294-v
GPR35a construct

Figure 2

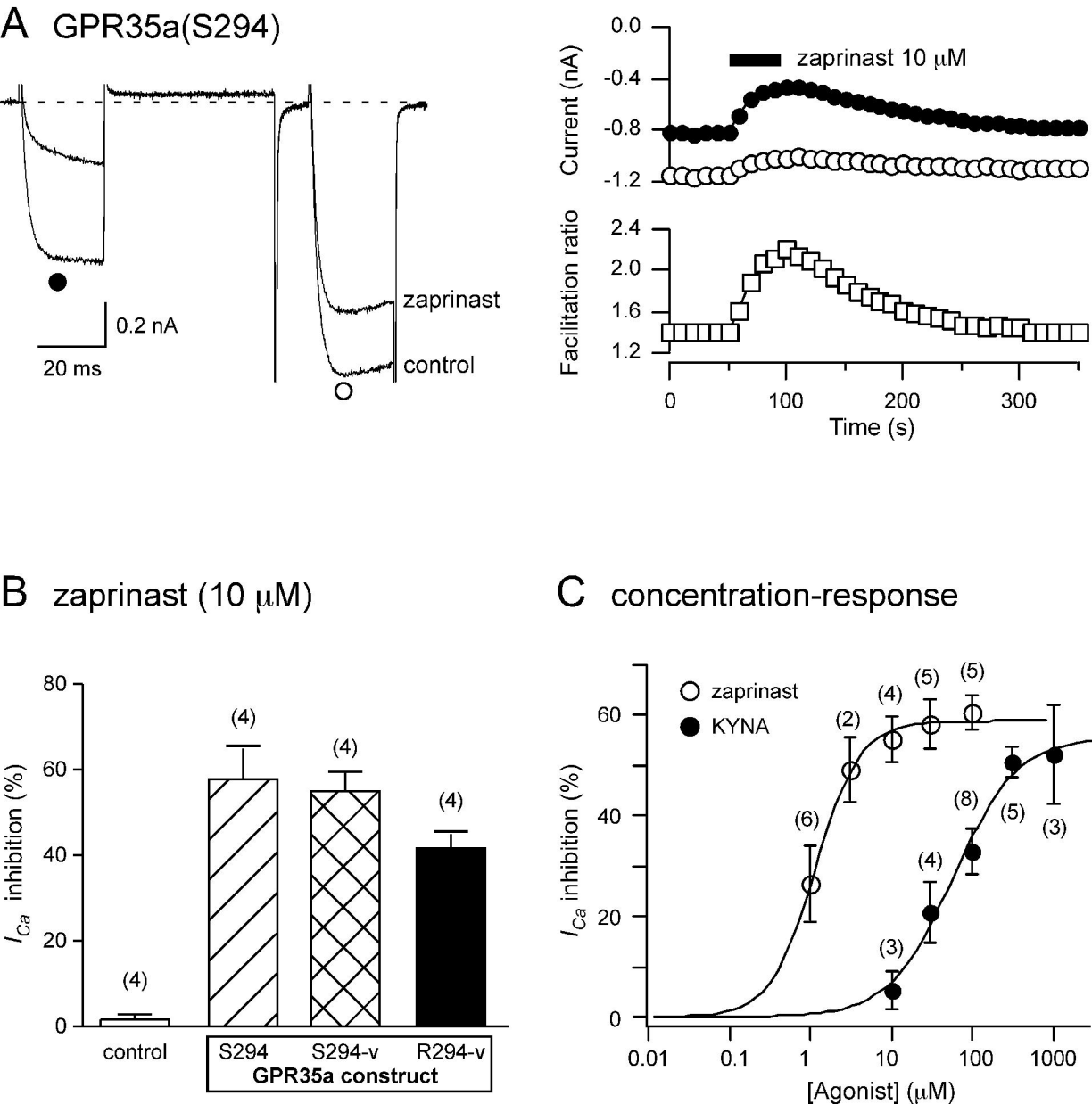
A GPR35a(S294)
0.2 nA
20 ms
zaprinast
control
zaprinast 10 μM
Current (nA)
0.0
-0.4
-0.8
-1.2
Facilitation ratio
2.4
2.0
1.6
1.2
0
100
200
300
Time (s)
B zaprinast (10 μM)
I_{Ca} inhibition (%)
80
60
40
20
0
(4)
(4)
(4)
(4)
control
S294
S294-v
R294-v
GPR35a construct
C concentration-response
zaprinast
KYNA
(6)
(2)
(4)
(5)
(5)
(3)
(4)
(8)
(5)
(3)
0.01
0.1
1
10
100
1000
[Agonist] (μM)

Figure 3

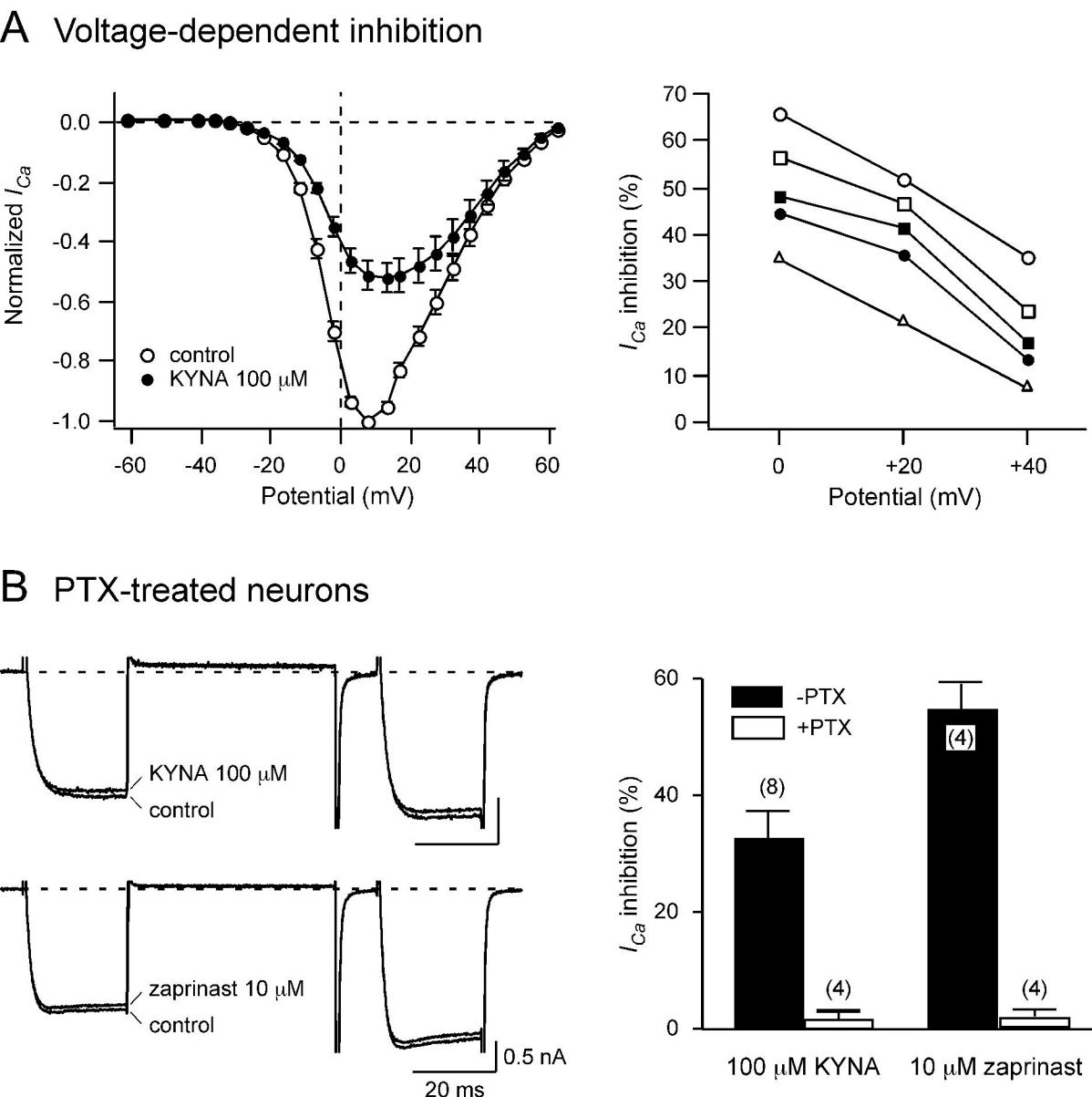
A Voltage-dependent inhibition
Normalized I_{Ca}
0.0
-0.2
-0.4
-0.6
-0.8
-1.0
control
KYNA 100 μM
-60
-40
-20
0
20
40
60
Potential (mV)
I_{Ca} inhibition (%)
70
60
50
40
30
20
10
0
0
+20
+40
Potential (mV)
B PTX-treated neurons
KYNA 100 μM
control
zaprinast 10 μM
control
0.5 nA
20 ms
I_{Ca} inhibition (%)
60
40
20
0
-PTX
+PTX
(8)
(4)
(4)
(4)
100 μM KYNA
10 μM zaprinast

Figure 4

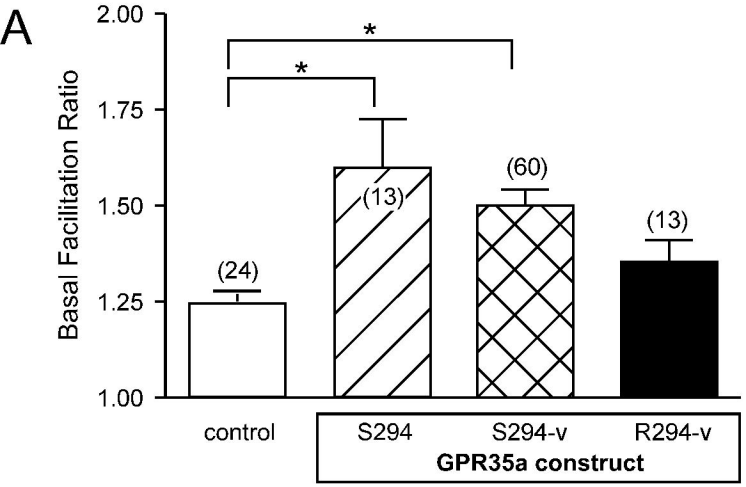
A
Basal Facilitation Ratio
2.00
1.75
1.50
1.25
1.00
*
*
(24)
(13)
(60)
(13)
control
S294
S294-v
R294-v
GPR35a construct

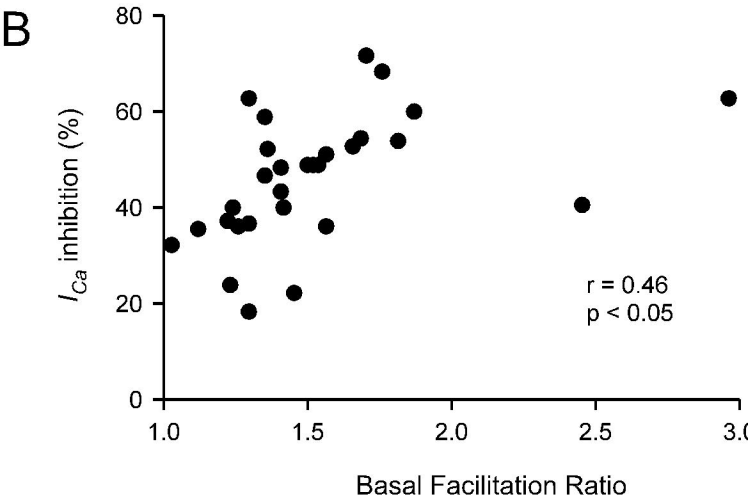
B
I_{Ca} inhibition (%)
80
60
40
20
0
r = 0.46
p < 0.05
1.0
1.5
2.0
2.5
3.0
Basal Facilitation Ratio

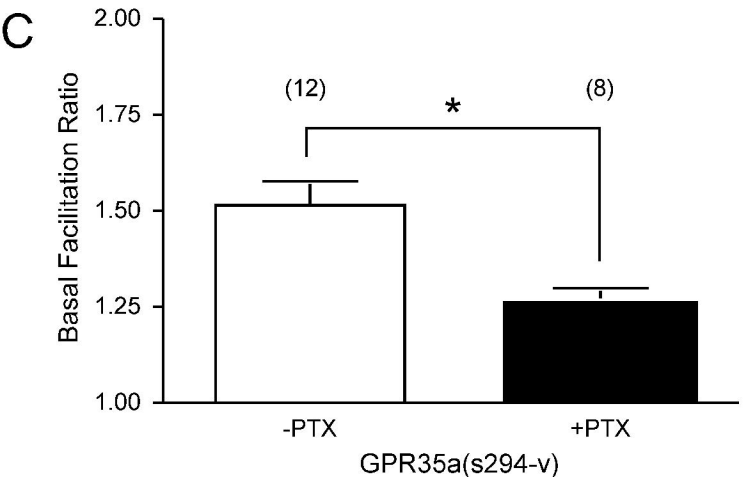
C
Basal Facilitation Ratio
2.00
1.75
1.50
1.25
1.00
(12)
*
(8)
-PTX
+PTX
GPR35a(s294-v)

Figure 5

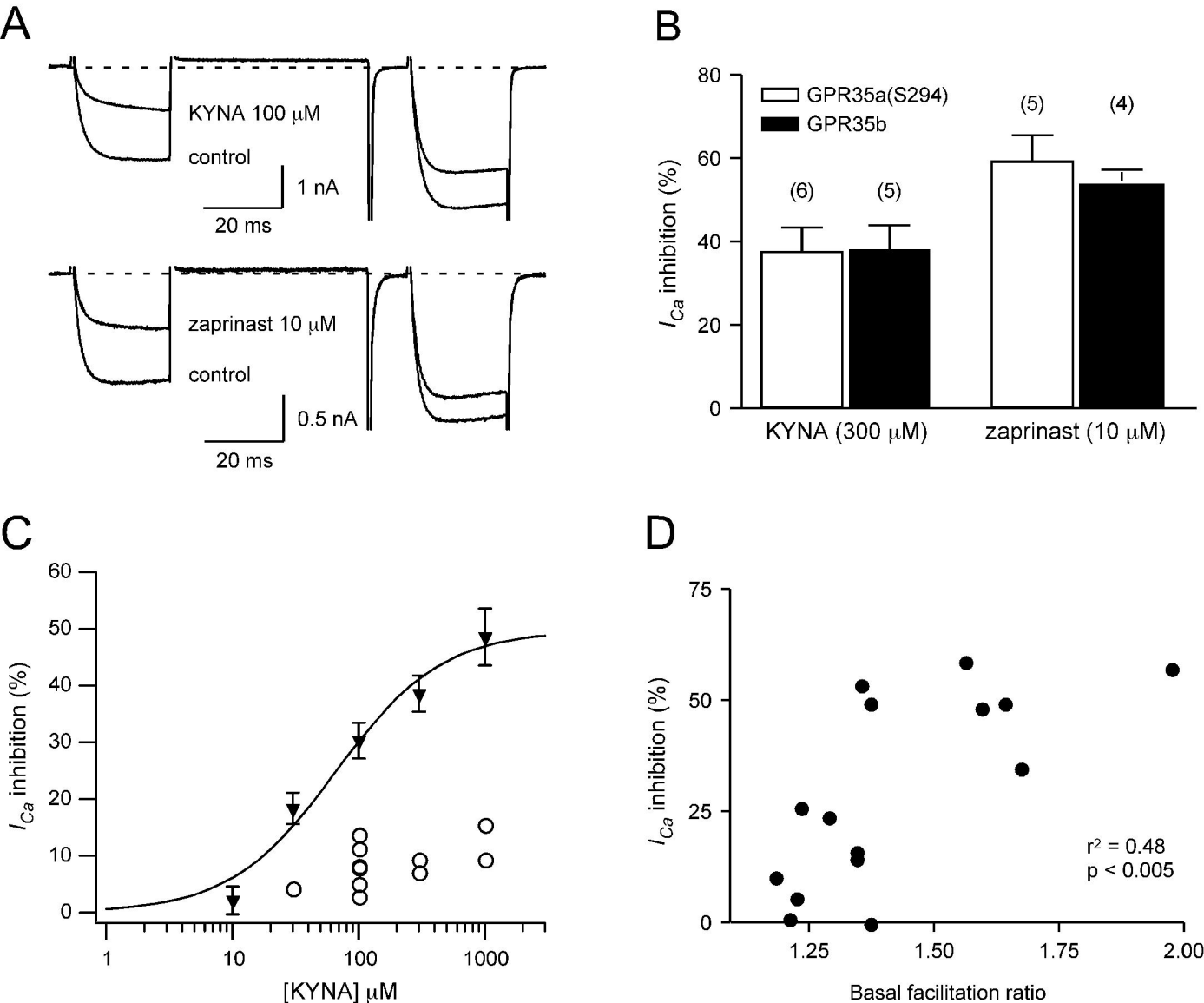
A
KYNA 100 μM
control
1 nA
20 ms
zaprinast 10 μM
control
0.5 nA
20 ms
B
GPR35a(S294)
GPR35b
(6)
(5)
(5)
(4)
I_{Ca} inhibition (%)
KYNA (300 μM)
zaprinast (10 μM)
C
I_{Ca} inhibition (%)
[KYNA] μM
D
I_{Ca} inhibition (%)
r^2 = 0.48
p < 0.005
Basal facilitation ratio

Figure 6